2018 IEEE Intelligent Vehicles Symposium (IV)
Changshu, Suzhou, China, June 26-30, 2018

Hazard-evaluation-based Driver-automation Switched Shared Steering Control for Intelligent Vehicles

Yangyang Guo[1 2], Jun Liu[1 2], Linhuan Song[1 2], Hongyan Guo[1 2⋆], Yunfeng Hu[1 2]and Hong Chen[1 2]

Abstract— **The driving model switched between an intelligent vehicle and a human driver is a hot discussing issue for intelligent driving system, and it relates to the safety of the intelligent vehicle and traffic efficiency of transportation system. It presents a hazard-evaluation-based driver-automation switched shared steering control approach for intelligent vehicles in this manuscript. The switched operation between human driver and autopilot system is carried out when the hazard situation is tested by the autopilot controller. The driver's operation and the deviation from the road center line are employed to carry out the hazard evaluation. The autopilot controller is designed using the constrained model predictive control (MPC) approach to keep the intelligent vehicle run in the safe area that is between the road boundary. In order to verify the control performance of the proposed algorithm, simulation verification under hazard situation of the proposed approach are carried out and compared with the non-switching method. The results show that the intelligent vehicle can keep safe in the hazard situation. .**

I. INTRODUCTION

Vehicles can bring convenience to people, but accidents can bring great disaster to people. According to the National Highway Traffic Safety Administration (NHTSA) in 2013 , there were 33,561 traffic deaths in the United States, and 2362,000 serious injuries occurred [1]. Intelligent vehicles can reduce the occurrence of accidents, the highest goal of intelligent vehicle is to realize autonomous driving. The American Society of Automotive Engineers (SAE) classifies the autonomous driving ranks as 5 grades [2]. There seems to be a consensus that fully autonomous driving will be on the road by 2030 [3]. At present, the intelligent vehicle can not carry out the autonomous driving of the whole condition, and the conditional man-machine driving power switching system refers to the switch between the human driving power and the autopilot system driving power in the specific scene. By the switching between the driver and the autopilot, the vehicle is safely driven.

A number of measures and metrics have been used to study the switch control of intelligent vehicles. Wada *et al*. study when the auto switch from automatic control to manual control for emergency steering and driving control of smooth switching requirements, they propose a switch from driving assistant system to the driver's smooth steering control method. The method of adjusting the steering control intensity based on the tactile sharing control technology is adopted. The effectiveness of this method is verified by experiments on micro electric vehicles [4]. Bahram *et al*. proposed a method to handle the driver takeover request in the process of automatic driving based on the model predictive control method. Allow the vehicle to park safely within a limited time of takeover or encounter potential stability and dangerous conditions [5]. Sheehan *et al*. proposed a bayesian network statistical risk estimation method, suitable for self-driving vehicles under two scenarios, the driver control and vehicle automatic control. This method is especially applicable to remote information processing data generated by vehicle inherent technology [6]. All of these people are working on switching methods, and here are some of the researchers' studies on how drivers respond to switch control.

Banks *et al*. studied whether some autonomous driving could reasonably serve as a monitoring driver for autonomous vehicles when they could not complete the monitoring task for a long time. Using the tesla S-model autopilot mode, collect image observation information as part of a study to the highway. The subject analysis of the image shows that, since the driver showed too much trust in the automatic controller, the driver did not get the appropriate support in the process of insisting on the monitoring responsibility [7]. Merat *et al*. use the head posture and eye movement information to monitor driver fixation point deviates from the middle of the road, to study the state of visual attention and the time required to take over the control features [8],[9]. Lv *et al*. proposed a method of using hybrid system to synchronously observe the state of the driver in the loop information physical system [10]. In addition, some researchers studied the timing of switching.

Nilsson *et al*. considered the question of when vehicle control should be safely transferred from autopilot to driver. Based on the description of the driver's ability to control the vehicle, a subset of the vehicle state space is defined, namely the concept of a controllable subset of the driver. By defining the limits of the normal driving envelope of the individual driver, the estimated boundary of the controllable subset of the driver is found. The vehicle model and reachability analysis are used to evaluate whether the vehicle's starting and maintaining state is in the controllable subset of the driver when vehicle control transfers from autopilot to driver. and the effectiveness of the method was verified by real vehicle experiment [11].

In this paper, a hazard-evaluation-based driver-automation switched shared steering control for intelligent vehicles is presented. The switch is based on the hazard index, which

1. State Key Laboratory of Automotive Simulation and Control, Jilin University, Changchun Jilin 130025 China, E-mail: guohy11@jlu.edu.cn
2. Department of Control Science and Engineering, Jilin University, Changchun Jilin 130025 China E-mail: chenh@jlu.edu.cn
⋆ Corresponding author.

includes the driver's operational hazard index and the road hazard index. The switch mode is composed of the driver mode and the autopilot mode. To design the autopilot controller, a constrainted MPC is adopted in this paper. When the driver's operational hazard index and the road hazard index are both more than the threshold, switch driver mode to autopilot mode. Otherwise, keep the driver mode.

The paper is organized as follows: In section II, the vehicle model is developed. Section III presents the two modes between the driver and the autopilot controller. Section IV describes the switch rules. Simulations are carried out to showing the controller performance in section V.

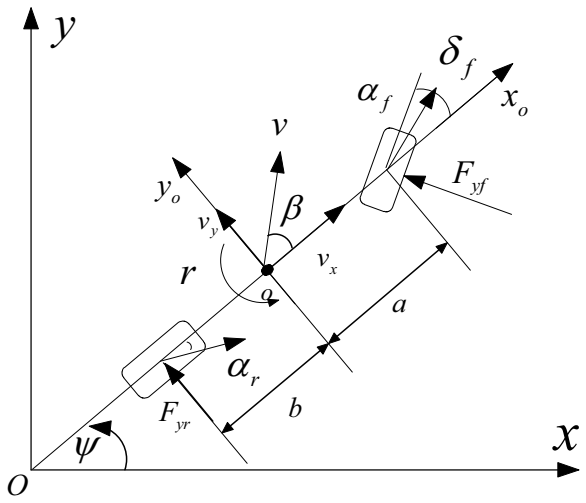

Fig. 1. Vehicle model

II. VEHICLE MODEL

A. Vehicle dynamic model

As shown in Fig. 1, the vehicle model is used to design the autopilot controller in the MPC scheme. It includes vehicle dynamics model and kinematics model. At the same time, it is of reference significance to driver's driving. This paper is concerned with the steering characteristics of the vehicle, so it is assumed that the longitudinal speed of vehicle is constant throughout the prediction horizon. A linear two-degree-of-freedom(dof) vehicle model is used in this paper. It not only characterizes the dynamics of the vehicle, but also because it's a typical second-order system, which response is optimal and can be used as a reference for the driver. According to the lateral force balance equation and the torque balance equation, we can obtain the expression of the linear 2-dof vehicle model as follows:

$$\begin{aligned}\dot{\beta} &= \frac{F_{yf}+F_{yr}}{mv_x} - r,\\ \dot{r} &= \frac{aF_{yf}-bF_{yr}}{I_z}.\end{aligned} \tag{1}$$

where F_{yf} is the lateral tire force of the front axle, F_{yr} is the lateral tire of the rear axle, m is the vehicle mass, v_x is the longitudinal velocity in the body fixed frame, I_z is the moment of inertia, a is the distance from the center of gravity to the front axle and b is the distance from the center of gravity to the rear axle. r is the yaw rate, β is the sideslip angle.

The tire force expression can be obtained by linearizing the tire model, so the front and rear lateral tire forces can be expressed as:

$$\begin{aligned}F_{yf} &= C_f\alpha_f,\\ F_{yr} &= C_r\alpha_r.\end{aligned} \tag{2}$$

where C_f and C_r represent the linearized cornering stiffness of the front and rear wheels. The tire slip angle in the front and rear can be approximated as:

$$\begin{aligned}\alpha_f &= \beta + \frac{ar}{v_x} - \delta_f,\\ \alpha_r &= \beta - \frac{br}{v_x}.\end{aligned} \tag{3}$$

where δ_f is the front wheel steering angle.

The state equation of the linear 2-dof vehicle model can be expressed as :

$$\begin{aligned}\dot{\beta} &= \frac{(C_f+C_r)}{mv_x}\beta + (\frac{(aC_f-bC_r)}{mv_x^2} - 1)r - \frac{C_f}{mv_x}\delta_f\\ \dot{r} &= \frac{(aC_f-bC_r)}{I_z}\beta + \frac{(a^2C_f+b^2C_r)}{I_zv_x}r - \frac{aC_f}{I_z}\delta_f.\end{aligned} \tag{4}$$

B. Vehicle kinematic model

As shown in Fig. 1, The position states of the vehicle include yaw angle (ψ), lateral position of the center of gravity in the inertial coordinate system (y) and lateral position of the center of gravity in the inertial coordinate system (x). According to plane geometry relationship, The equations of motion of the position states can be expressed as:

$$\begin{aligned}\dot{\psi} &= r\\ \dot{y} &= v_x sin(\psi) + v_y cos(\psi)\\ \dot{x} &= v_x cos(\psi) + v_y sin(\psi).\end{aligned} \tag{5}$$

Because of β and ψ are changing in a small range, the sideslip angle can be approximated as: $\beta = \frac{v_y}{v_x}$, the motion of the y and x can be approximated as:

$$\begin{aligned}\dot{y} &= v_x\psi + v_x\beta\\ \dot{x} &= v_x.\end{aligned} \tag{6}$$

Combining (4) ,(5) and (6), selecting δ_f as the control variable u and choosing $[y\ \psi\ r\ \beta]$ as the state variable x, a continuous state-space function of the vehicle dynamic and kinematic model can be expressed as:

$$\dot{\mathrm{x}} = \mathrm{Ax} + \mathrm{B}u. \tag{7}$$

$$\mathrm{y} = \mathrm{Cx} \tag{8}$$

with

$$\mathrm{A} = \begin{bmatrix} 0 & v_x & v_x & 0\\ 0 & 0 & 0 & 1\\ 0 & 0 & \frac{aC_f-bC_r}{I_z} & \frac{a^2C_f+b^2C_r}{I_zv_x}\\ 0 & 0 & \frac{C_f+C_r}{mv_x} & \frac{aC_f-bC_r}{mv_x^2}-1 \end{bmatrix}, \mathrm{B} = \begin{bmatrix} 0\\ 0\\ -\frac{aC_f}{I_z}\\ -\frac{C_f}{mv_x} \end{bmatrix}, \tag{9}$$

$$\mathrm{C} = \begin{bmatrix} 1 & 0 & 0 & 0 \end{bmatrix}.$$

By discretizing the Eq. (7) and Eq. (8) using zero-order hold, a discrete-time model described as follows is obtained:

$$\mathrm{x}(k+1) = \mathrm{A_d x}(k) + \mathrm{B_d}u(k), \tag{10}$$

$$\mathrm{y}(k) = \mathrm{C x}(k). \tag{11}$$

with $\mathrm{A_d} = \mathrm{e}^{\mathrm{AT_s}}, \mathrm{B_d} = \int_0^{\mathrm{T_s}} \mathrm{e}^{\mathrm{A}\tau}\mathrm{d}\tau \cdot \mathrm{B}$, T_s is the sampling time.

III. SWITCH MODE

There are two modes for switching, one is the driver mode and the other is the autopilot mode. The driver mode is people to control the vehicle. The autopilot mode is the autopilot controller to control the vehicle. This paper uses the constraint MPC to design the autopilot controller. The goal of the autopilot controller is to make the vehicle track the center line of the road, which is considered to be the safest when the vehicle is driven along the center line of the road. At the same time, we must ensure that the vehicle does not exceed the road boundary. the system control diagram show as Fig. 2.

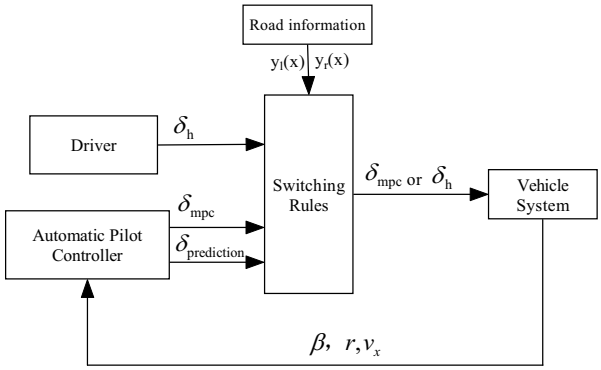

Fig. 2. System control block diagram

Define the control input sequence U(k) at the time k as:

$$\mathrm{U(k)} = \begin{bmatrix} u(k) \\ u(k+1) \\ \vdots \\ u(k+N-1) \end{bmatrix} \tag{12}$$

where N is the control horizon. P is the predictive horizon, $P \geq N$, and $u(k+N-1) = u(k+N) = \cdots = u(k+P-1)$, then based on Eq. (7), the predict state of the system at the k can be written as:

$$\mathrm{x(k+\ 1)} = \mathrm{A_c x(k)} + \mathrm{B_c u(k)} \tag{13a}$$

$$\vdots$$

$$\mathrm{x(k+N)} = \mathrm{A_c^N x(k)} + \mathrm{A_c^{N-1} B_c u(k)} + \cdots + \mathrm{B_c u(k+N-1)} \tag{13b}$$

$$\vdots$$

$$\mathrm{x(k+P)} = \mathrm{A_c^P x(k)} + \mathrm{A_c^{P-1} B_c u(k)} + \cdots + \sum_{\mathrm{i=1}}^{\mathrm{P-N+1}} \mathrm{A_c^{i-1} B_c u(k+N-1)} \tag{13c}$$

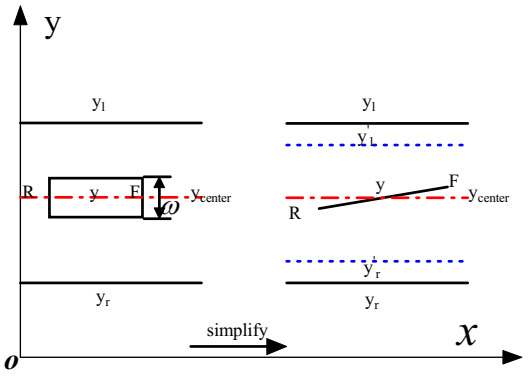

Fig. 3. Vehicle and road simplified schematic

Through the reasonable simplification of vehicles and road boundaries, which show as Fig. 3, $y(k+i)$ is considered to satisfy the following constraints:

$$y_l(k+i) - \frac{w}{2} - L_F\psi(k+i) \leq y(k+i) \tag{14a}$$

$$y(k+i) \leq y_r(k+i) + \frac{w}{2} - L_F\psi(k+i) \tag{14b}$$

$$y_l(k+i) - \frac{w}{2} + L_R\psi(k+i) \leq y(k+i) \tag{14c}$$

$$y(k+i) \leq y_r(k+i) + \frac{w}{2} + L_R\psi(k+i) \tag{14d}$$

where $y_l(k+i)$ and $y_r(k+i)$ are discrete values of the road boundaries. $y_{center}(k+i)$ is the center line of the road. L_F is the distance between the front and center point of the vehicle. L_R is the distance between the rear and center point of the vehicle. w is the width of the vehicle. $\psi(k+i) = [0\ 1\ 0\ 0]\mathrm{x}(k+i)$, $i = 1, \cdots, P$.

To track the center line of the road is an important task of MPC controller. it can be achieved by minimizing the following objective function:

$$J_1 = \sum_{i=1}^{P} (y(k+i) - y_{center}(k+i))^2 \tag{15}$$

where $Y_{center}(k+i) = (y_l(k+i) + y_r(k+i))/2$.

To keep the car steady, the β should be as small as possible, and to ensure riding comfort, the Δu(k) should be as small as possible. it can be achieved by minimizing the following objective function:

$$J_2 = \Gamma_1 \sum_{i=1}^{P} (\beta(k+i))^2 + \sum_{i=1}^{P-1} (\Delta u(k+i))^2 \tag{16}$$

where Δu(k+i)=u(k+i)-u(k+i-1). The ultimate cost function can be expressed as:

$$\begin{aligned} J = \Gamma_2 \sum_{i=1}^{P} (y(k+i) - Y_{center}(k+i))^2 + \\ \Gamma_1 \sum_{i=1}^{P} (\beta(k+i))^2 + \sum_{i=1}^{P-1} (\Delta u(k+i))^2 \end{aligned} \tag{17}$$

where Γ_1 and Γ_2 are the weighting factor to deal with the demands of each optimization objective so that the most suitable result can be obtained.

So the autopilot controller can be described as the following optimization problem:

$$\begin{aligned} &\min_{\mathrm{U(k)}} J = \Gamma_2 J_1 + J_2 \\ &\textbf{s.t.} \quad \mathrm{Eq.}(14a) - \mathrm{Eq.}(14d) \end{aligned} \tag{18}$$

IV. SWITCHING RULES

In this paper, two kinds of indicators are given to evaluate the current driving hazard index of vehicle. One is the driver's operational hazard index that is the deviation between the driver's current steering wheel angle and the next moment desired angle. The other is the road hazard index that is the deviation between the current driving position of the center of gravity and the center line of the road. The desired angle $\delta_{prediction}$ at the next moment is predicted by the autopilot controller. The road information hypothesis is already known. The driver's operational hazard index can be expressed as

$$E_{driver}(k) = \delta_h(k) - \delta_{prediction}(k). \tag{19}$$

where $\delta_h(k)$ is the driver's input. $\delta_{prediction}(k)$ is the value that the next moment is expected. k is the current moment.

The road hazard index can be expressed as:

$$E_{road}(k) = y(k) - y_{center}(k). \tag{20}$$

where $y(k)$ is the position of the center of gravity of the vehicle, y_{center}(k) is the center line of the road.

In theory, the greater difference between the actual value and the expected value, the more dangerous. The driver's operational hazard index and the road hazard index both have an appropriate threshold. When The driver's operational hazard index and the road hazard index are both more than their threshold, we think the situation is dangerous. Then switch from the driver mode to the autopilot mode.

V. SIMULATION VALIDATION

In order to test the effect of autopilot controller and driver switching, a high precision vehicle simulation software veDYNA is adopted in this paper. The veDYNA's vehicle simulation type used in this paper is the HQ430. The parameters for this model are specified in Table I. Controller parameters are specified in Table II.

TABLE I

HQ430 VEHICLE PARAMETERS

Symbol	Unit	Value	Symbol	Unit	Value
m	kg	2160	I_z	$\mathrm{kg \cdot m^2}$	3411.52
a	m	1.5	C_f	N/rad	−87594
b	m	1.35	C_r	N/rad	−87594

TABLE II

AUTOPILOT CONTROLLER PARAMETERS

Symbol	meaning	Value	Symbol	meaning	Value1
N	*control horizon*	25	T_m	*duration*	0.02
P	*prediction horizon*	25	Γ_1	*weight*	100
T_s	*sampling time*	0.001	Γ_2	*weight*	5

Fig. 4 shows that when the driver is driving alone, the vehicle goes beyond the road boundary. But under the same conditions switch from the driver to the autopilot controller, which make the vehicle run in the road boundary. By comparing the phase plane that is composed of β and r, it can be seen that the vehicle state is completely different in two situations. The former vehicle has lost its stability, while the latter keeps the vehicle stable, but it can be seen that the phase plane changes more frequently, indicating that the switching frequency is so fast that the vehicle shaking.

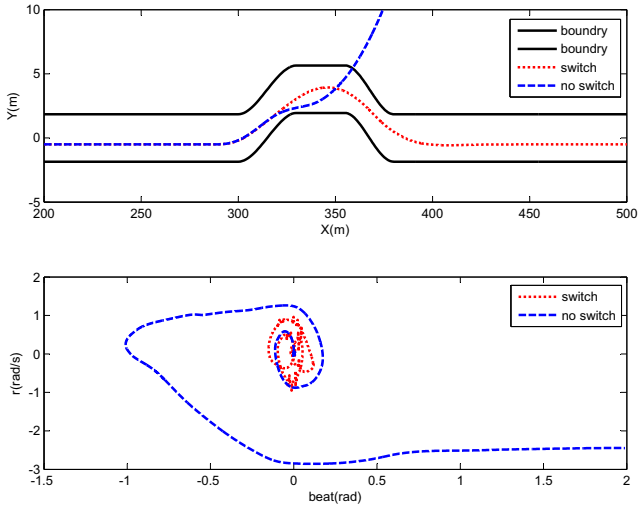

Fig. 4. The comparison between switch and non-switching stability

Fig. 5 shows the comparison between the driver's angle and the switching angle, and also gives the switching flag. When the switching flag changes from 0 to 1, the situation is judged to be dangerous. The driver switches to the autopilot

controller and the driver's angel is not input to the vehicle. When flag is changed from 1 to 0, it switches from autopilot controller to driver. At this point the angle of the autopilot controller is no longer input to the vehicle. Flags can also be seen to switch too frequent between 18 and 19 seconds. This is bad for vehicle.

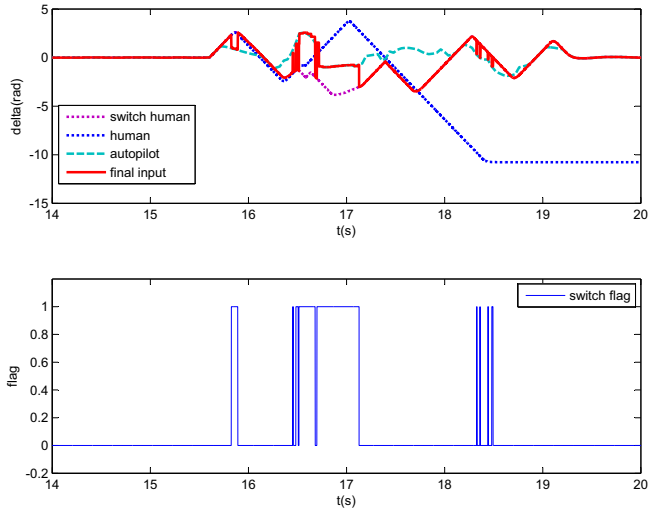

Fig. 5. The comparison between switch and non-switching's control

In order to solve the problem of too frequent switching, this paper adopts a method to suppress frequent switching. The sampling time is 0.001s in this paper. If the switch occurs, let the mode persist for 0.02s. This effectively avoids switching from one mode to the other quickly. Fig. 6 shows the vehicle status obtained by switch2 compared with the switch1. Both methods can keep the vehicle stable on the road boundary.

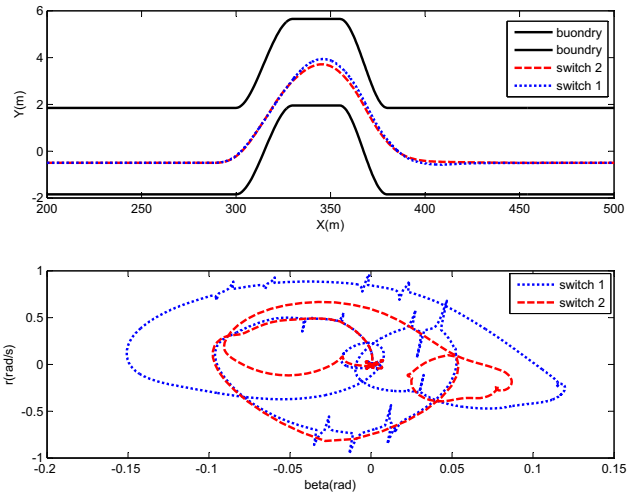

Fig. 6. Vehicle status comparison

However, by comparing the phase plane, it can be seen that the plane curve of the method with switch2 is smoother and the range of variation is smaller. Further by Fig. 7 ,the control input of switch2 is more smooth than switch1, and the number of switches is significantly reduced compared to switch1.

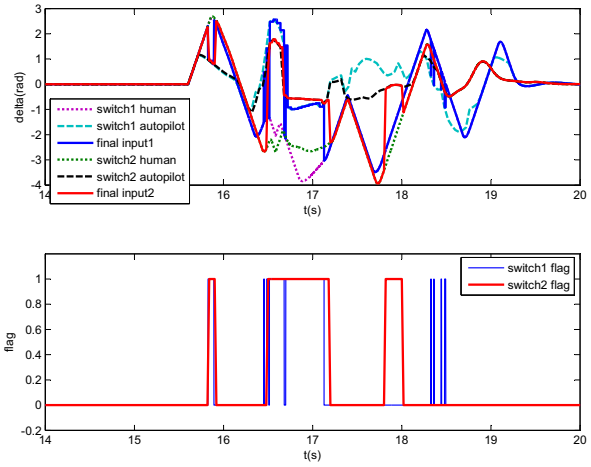

Fig. 7. Control input and switch status comparison

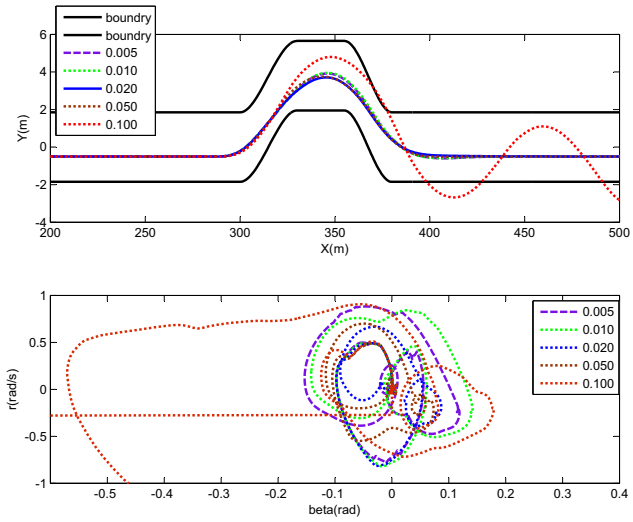

Fig. 8. Comparison of vehicle status in different mode duration

Fig. 8 shows the impact of the different duration of the mode on switching control. When the duration time is 0.1s, the vehicle drives out of the road boundary. The reason why the vehicle drives out of the road boundary is that the driver switch to the autopilot controller, which has exceeded the controller's adjustment range. The phase diagram also shows that the vehicle is in a state of instability when the mode duration is 0.1s. Fig. 9 shows the control input and switch flag at different mode duration. if the mode duration is too short, frequent switching is not restrained. proper mode duration can restrain frequent switching; but a long mode duration can make vehicle instability. So we should select

the mode duration appropriately. The duration of the mode selected in this article is 0.02 seconds.

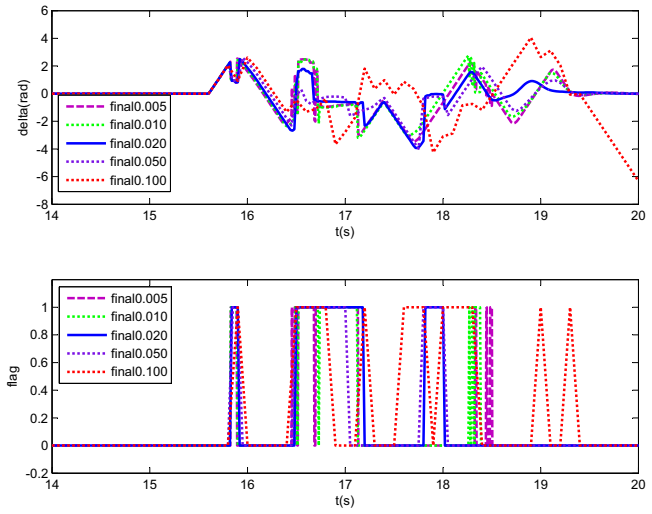

Fig. 9. Different mode duration input and switching state contrast

VI. CONCLUSIONS

This paper presents a hazard-evaluation-based driver-automation switched shared steering control for intelligent vehicles. The autopilot controller is designed by a constraint MPC method. The hazard-evaluation includes the driver's operational hazard index and the road hazard index. The results of simulation show that when the situation is danger, the driver mode can switch to the autopilot mode automatically to make the vehicle safe driving. when the situation is safe, the autopilot mode will switch to the drive mode.

ACKNOWLEDGMENT

This work is supported by the National Nature Science Foundation of China (61403158, 61520106008,61790564, U1664263).

REFERENCES

[1] Administration NHTS. Traffic safety facts 2013: A compilantion of motor vehicle crash data from the fatality analysis reproting system and the general estimates system[R]. Washington, DC: National Highway Traffic Safety Administration, 2013.

[2] SAE International, 2014. Taxonomy and Definitions for Terms Related to Onroad Motor Vehicle Automated Driving Systems (Standard No. J3016). Retrievedfrom. SAE International.

[3] M. Kyriakidis, R. Happee and JCFD. Winter, Public opinion on automated driving: results of an international questionnaire among 5000 respondents, Transp. Res. Part F Traffic Psychol,vol.32, pp.127140,2015.

[4] Wada T, Sonoda K, Okasaka T, et al. Authority transfer method from automated to manual driving via haptic shared control[C]. IEEE International Conference on Systems, Man, and Cybernetics. IEEE, 2017.

[5] Bahram M, Aeberhard M, Wollherr D. Please take over! An analysis and strategy for a driver take over request during autonomous driving[C]. Intelligent Vehicles Symposium. IEEE,pp.913919,2015.

[6] Sheehan B, Murphy F, Ryan C, et al. Semi-autonomous vehicle motor insurance: A Bayesian Network risk transfer approach[J]. Transportation Research Part C Emerging Technologies, vol.82,pp.124137,2017.

[7] Banks V A, Eriksson A, O'Donoghue J, et al. Is partially automated driving a bad idea? Observations from an on-road study[J]. Applied Ergonomics, vol.68,pp.138145,2018.

[8] Merat N, Jamson H, et al. Highly automated driving, secondary task performance, and driver state[J]. Human Factors, vol.54,no.5, pp.762771,2012

[9] Merat N, Jamson H, et al. Transition to manual: driver behaviour when resuming control from a highly automated vehicle[J]. Transportation Research Part F: Traffic Psychology and Behaviour, vol.27,no.8, pp.274282,2014.

[10] Lv, C., Liu, Y., Hu, X., Guo, H., Cao, D., and Wang, F. Y. "Simultaneous Observation of Hybrid States for Cyber-Physical Systems: A Case Study of Electric Vehicle Powertrain." IEEE Transactions on Cybernetics, 2017, in press.

[11] Nilsson J, Falcone P, Vinter J. Safe Transitions From Automated to Manual Driving Using Driver Controllability Estimation[J]. IEEE Transactions on Intelligent Transportation Systems,vol.16 no.4 pp.18061816,2015.